Bull. Mater. Sci., Vol. 31, No. 6, November 2008, pp. 869–876. © Indian Academy of Sciences.

Study of effect of composition, irradiation and quenching on ionic conductivity in $(PEG)_x : NH_4NO_3$ solid polymer electrolyte

R DAMLE*, P N KULKARNI and S V BHAT†

Department of Physics, Bangalore University, Bangalore 560 056, India
†Department of Physics, Indian Institute of Science, Bangalore 560 012, India

MS received 31 January 2008; revised 29 April 2008

Abstract. **We have prepared, characterized and investigated a new PEG-2000 based solid polymer electrolyte $(PEG)_x$: NH_4NO_3. Ionic conductivity measurements have been made as a function of salt concentration as well as temperature in the range 265–330 K. Selected compositions of the electrolyte are exposed to a beam of 8 MeV electrons and ^{60}Co γ-rays to an accumulated dose of 10 kGy to study the effect on ionic conductivity. The electrolyte samples are also quenched at liquid nitrogen temperature and conductivity measurements are carried out. The ionic conductivity at room temperature exhibits a characteristic peak for the composition, $x = 46$. Electron beam irradiation results in an increase in conductivity for all compositions by a factor of 2–3. Exposure to γ-rays enhances the conductivity by one order of magnitude. Quenching at low temperature has resulted in an increase in conductivity by 1–2 orders of magnitude. The enhancement of conductivity upon irradiation and quenching is interpreted as due to an increase in amorphous region and decrease in crystallinity of the electrolyte. DSC and NMR measurements also support this conclusion.**

Keywords. **Solid polymer electrolytes; ionic conductivity; effect of ionizing radiation.**

1. Introduction

Solid polymer electrolytes (SPEs) are the subject of intensive study owing to their applications in solid state rechargeable batteries. The key problem with SPEs is the low conductivity at ambient temperature. In recent years, several different strategies have been employed to enhance the ionic conductivity and cation transport number. To date, polyethylene oxide (PEO) and polyethylene glycol (PEG) based polymer electrolytes have been regarded as some of the most suitable electrolytes for rechargeable batteries. Most of the studies of concentration and temperature dependence and enhancement of conductivity have been on high molecular weight polymers (e.g. PEO) complexed with alkali metal salts (lithium being the most studied) (Armand *et al* 1979; Gray 1991; Nader and Bhat 1996, Binesh and Bhat 1999; Joykumar Singh and Bhat 2003). However, much attention has not been paid to the somewhat low molecular weight (MW ~ 2000) PEOs or PEGs. PEG has the same monomeric unit as PEO but has an end hydroxyl group, with the chemical formula: H $(–CH_2–CH_2–O–)_n$–OH. Shi and Vincent (1993) studied the effect of molecular weight of polymers on cation mobility and have shown that above a critical limit of 3200, the MW has no significant effect on cation mobility. However, below this limit due to different viscosity and diffusion behaviours, an additional transport mechanism could be operating. In this low molecular weight region, referred to as the 'Rouse region', there is a possibility of the polymer chain diffusion besides the segmental motion. Keeping these in mind, PEG of molecular weight 2000 was chosen for the preparation of a new SPE: $(PEG)_x : NH_4NO_3$. The PEG (MW = 2000) used in our studies, is a solid at room temperature having the melting point close to 50°C. It has 46 repeat units ($n = 46$) and is highly crystalline. The salt, NH_4NO_3, has been chosen as it fulfils the electrochemical stability criteria (Vincent 1987). It has low lattice energy (637 kJ mol^{-1}) (Jenkins and Morris 1976; Haig *et al* 2004) and NH_4^+ is a cation with small radius (1·4 Å), which is favourable for the polymer salt complex formation. Also NO_3^{-1} is a large soft anion having low charge density, which helps in reducing the ion-pair formation with NH_4^+. It is generally known that conductivity in SPEs is influenced by the concentration of defects, their mobility and also the fraction of the amorphous region in the system (Berthier *et al* 1983). There are several ways of increasing the amorphous region/defect concentration and hence the ionic conductivity viz. exposing these materials to high energy ionizing radiation, quenching and addition of plasticizers to the electrolytes. We report here the effect of 8 MeV electron and ^{60}Co γ-ray irradiation and quenching at low temperature on the ionic conductivity of $(PEG)_x$: NH_4NO_3 polymer salt complex.

*Author for correspondence (ramkrishnadamle@bub.ernet.in)

2. Experimental

The chemicals, polyethylene glycol (PEG) of mol. wt. 2000 (Fluka) and NH_4NO_3 (Fluka), were used without further purification. The $(PEG)_x : NH_4NO_3$ complexes (in the composition x = 15, 20, 30, 46, 70, 100, 150, 200, 300 and 400 where x is ratio of number of ether oxygen in one monomer unit of the polymer to each NH_4^+ ion of the salt) were prepared by the standard solution cast method using methanol as the common solvent (Nader and Bhat 1996). The samples with higher salt concentrations are softer and moderately hygroscopic. Samples of intermediate salt concentrations are harder and less hygroscopic. All the samples are dried under vacuum for several hours before using them for measurements. The X-ray diffraction (XRD) patterns were recorded using a Scintag XDS 2000 diffractometer at a scan rate of 10°/min. Differential scanning calorimetry (DSC) measurements were carried out on a MDSC 2920 (TA Instruments, USA) in standard mode. 10–12 mg of the sample was used for the DSC recording. Samples were heated to 100°C at the rate of 10°C/min followed by cooling to –100°C. The recordings were done in heating as well as in cooling cycles. Room temperature ^{1}H nuclear magnetic resonance (NMR) line width measurements were carried out on a Bruker DSX-300 spectrometer operating at 300 MHz frequency. A single 90° pulse of 4 μs was used with 0·5 s recycle delay. ^{1}H NMR line width measurements were also carried out in the temperature range 200–340 K for a few compositions to study motional narrowing. Ionic conductivity measurements were carried out using a dual phase lock-in-amplifier (PAR-5210) by complex impedance method. For conductivity measurements, the samples were cast into Teflon rings (diameter ~7 mm, thickness ~1–2 mm) and the conductivity, σ, was determined using the relation, $\sigma = l/AR$, where l and A are the thickness and area of the sample, respectively and R the bulk resistance determined from the impedance plot. Ionic conductivities were also measured as a function of temperature in the range 265–330 K using liquid nitrogen gas flow cryostat described elsewhere (Nader and Bhat 1996; Binesh and Bhat 1999; Joykumar Singh and Bhat 2003). To study the effect of ionizing radiation on ionic conductivity, selected compositions of the samples were exposed to a beam of 8 MeV electrons and ^{60}Co γ-rays (energy, 1·08 MeV) to an accumulated dose of 10 kGy and conductivity measurements were done immediately thereafter. Electron beam irradiation was carried out at the Variable Energy Microtron Centre, Mangalore University, Mangalore. ^{60}Co γ-ray irradiation was carried out using BRIT-2000 Blood Irradiator at ISRO Satellite Centre, Bangalore. To study the effect of quenching, the sample was heated to its melting point of about 40–45°C and liquid nitrogen was poured on to the molten sample. The rate of quenching was about 20–25°C/s.

Since the samples with higher salt concentration are hygroscopic, there is a possibility of moisture contamination. Hence the samples were repeatedly dried under vacuum and conductivity measurements were done to verify the reproducibility of the conductivity values. Consistent values of conductivity obtained after repeated vacuum drying ruled out the possibility of water contamination. All the conductivity values reported were within an error margin of 5%.

3. Results and discussion

3.1 *XRD measurements*

Figure 1 shows the XRD patterns for a few salt compositions of the polymer–salt complexes, as well as that for pure PEG and pure NH_4NO_3 salt. Two prominent peaks of PEG (at 2θ = 19·2 and 23·4°) are present in all the patterns indicating the presence of pure polymer in all. The NH_4NO_3 peaks are seen in none of the polymer–salt complexes and this signifies that the NH_4NO_3 solvates very well in PEG-2000 matrix. The intensity of the PEG peaks decreases at high salt concentrations. The diffraction peaks of the pure salt are absent in the polymer salt complexes indicating the absence of pure salt phase in these complexes.

3.2 *DSC measurements*

Figure 2 shows the DSC curves (endothermic) registered for $(PEG)_x : NH_4NO_3$ (x = 15, 46, 70 and 100). The summary of the DSC results for the heating cycle is given in table 1. The signal to noise ratio of the signature of glass transition temperature, T_g, in DSC is usually poor. Hence the T_g's were determined by fitting the traces to appropriate function using the software available with the instru-

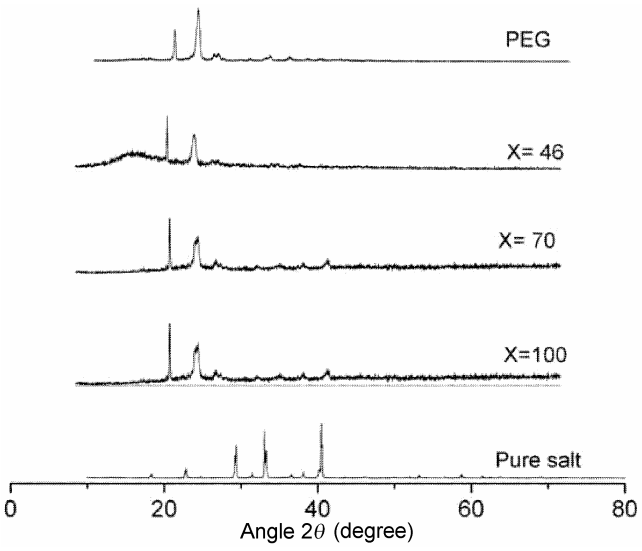

Figure 1. Powder XRD patterns of $(PEG)_x : NH_4NO_3$.

Table 1. DSC results of $(PEG)_x : NH_4NO_3$.

x	Salt (mole)	T_m (°C)	T_g (°C)	ΔH_m (J/g)	% Crystallinity (X_c)
15	3·067	53·8	–63·30 ± 1·0	125·1	61
20	2·300	53·9	–62·80 ± 1·0	131·2	64
30	1·533	53·1	–62·70 ± 1·0	133·1	66
46	1·000	53·7	–66·0 ± 1·0	136·0	67
70	0·657	54·4	–62·80 ± 1·0	135·0	68
100	0·460	53·3	–63·00 ± 1·0	142·1	70
200	0·230	54·1	–62·00 ± 1·0	158·0	78
400	0·115	54·7	–58·13 ± 1·0	160·3	79
PEG	0·000	55·0	–	168·0	83

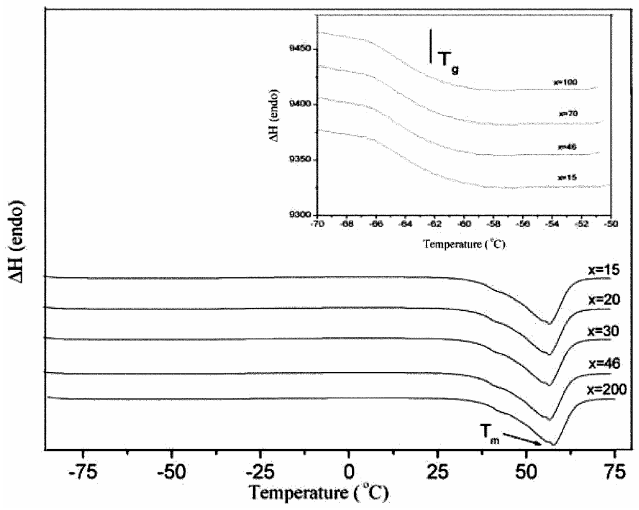

Figure 2. DSC traces (endothermic) of $(PEG)_x : NH_4NO_3$. Inset shows the relevant regions magnified.

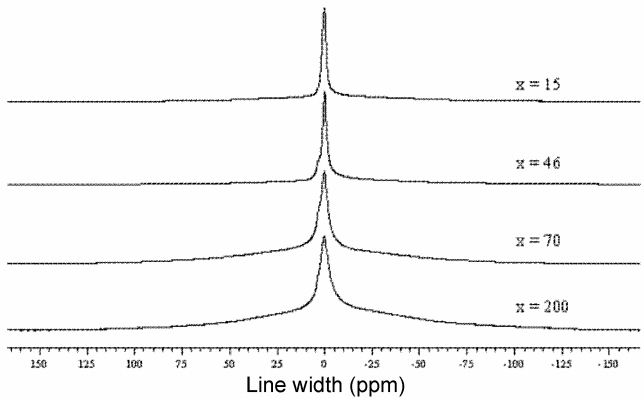

Figure 3. Room temperature ^{1}H NMR signals of $(PEG)_x$: NH_4NO_3 system (x = 15, 46, 70 and 200).

ment. The fitting error is indicated in table 1 and is the uncertainty in the T_g values. An increase in the glass transition temperature, T_g, with an increase in the salt concentration was observed and this signifies that the flexibility of the polymer chains decreases with an increase in the salt concentration in the polymer system. This reduction in flexibility of chains is usually interpreted as being a result of the effects of an increase in intramolecular and intermolecular coordinations between coordinating sites on the same or different polymer chains caused by the ions acting as transient cross links (Le Nest 1988). Melting temperature, T_m, of SPE system decreases as the salt content increases.

The enthalpy of melting, ΔH_m, is less for the SPEs in comparison with that of pure PEG-2000. The crystallinity fraction of pure PEG from NMR results is about 83%. The enthalpy of melting of pure PEG from DSC was observed to be 168 J/g. The enthalpy of melting of pure PEG was scaled up to 100% crystallinity and found to be 202·41 J/g (Li and Hsu 1984). The area under the curve for the melting endotherm is related to the crystallinity of the specimen. The percentage or the degree of crystallinity, X_c, in the sample was estimated from the ratio of the enthalpy, ΔH_m, of the samples and the enthalpy of melting of 100% crystalline PEG (ΔH_m PEG = 202·41 J/g). X_c decreases as the salt concentration increases (table 1). With an increase in NH_4NO_3 salt concentration, ΔH_m decreases indicating a decrease in the X_c (Watanabe *et al* 1984). Similar results have been obtained in PEG_x – $LiClO_4$ SPE also (Joykumar Singh and Bhat 2003). The reduction in the crystalline fraction, X_c, with the increase in the salt concentration can be attributed to the inhibition of crystallization by the salt.

3.3 *^{1}H NMR results*

The ^{1}H NMR spectra for low salt composition ($x > 150$) and for pure PEG consist of two components, a strong broad signal and a relatively narrow and weaker signal on top of it (figure 3). For the higher salt concentration ($x < 150$), the broad component merges with the baseline. Other workers also have observed this feature earlier as well (Hikichi and Furuichi 1965; Johansson *et al* 1992). It is generally known that the broad component is due to the crystalline regions and the narrow component corresponds to the amorphous regions. A Gaussian curve fits to the broad signal and a Lorentzian to the narrow signal. Figure 4 shows the variation of ^{1}H NMR line width as a function of salt concentration. As the salt concentration

increases, the line width decreases sharply in a similar way to the decrease in T_g as observed in DSC measurements and reaches a minimum at around $x = 46$ and then increases. Further increase in line width with salt concentration though X_c decreases could be due to the decrease in polymer chain flexibility as indicated by an increase in T_g at higher salt concentration. ^{1}H NMR signals for few selected compositions of $(PEG)_x : NH_4NO_3$ have been recorded as a function of temperature in the range 200–330 K. Figure 5 exhibits the variation of ^{1}H NMR line widths as a function of temperature. From the line width data, correlation times, τ_cs, have been calculated using the equation (Hendrickson and Bray 1973)

$$\tau_c = \frac{1}{\alpha\pi\Delta\nu} \times \tan\left[\frac{\pi}{2} \times \left(\frac{(\Delta\nu)^2 - (\Delta\nu_r)^2}{(\Delta\nu_d)^2 - (\Delta\nu_r)^2}\right)\right], \quad (1)$$

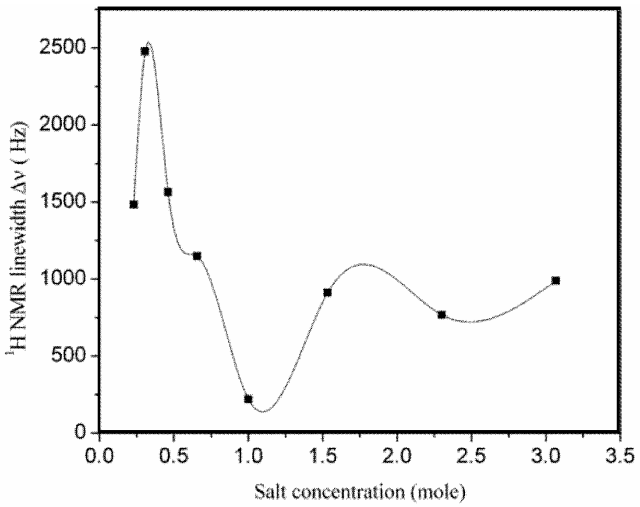

Figure 4. Room temperature ^{1}H NMR line widths vs salt concentration for $(PEG)_x : NH_4NO_3$ system.

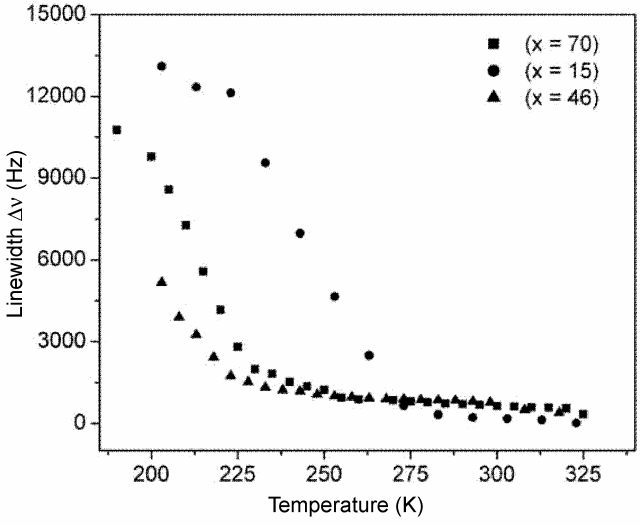

Figure 5. ^{1}H NMR line widths vs temperature plot for $(PEG)_x : NH_4NO_3$ system.

where τ_c is the correlation time, α a parameter of order unity, $\Delta\nu$ the line width in the narrowing region (in Hz), $\Delta\nu_r$ the residual line width and $\Delta\nu_d$ the rigid lattice linewidth. τ_cs are calculated at various temperatures. From the slope of the $\ln\tau_c$ vs $1000/T$ plot, E_a and τ_o are estimated. The ionic conductivity, σ(NMR), is also calculated using the Nernst–Einstein relation

$$\sigma(NMR) = \frac{Nq^2d^2}{6\tau_c kT}, \quad (2)$$

where N is the ammonium ion concentration per unit volume, d the average ionic jump distance and q the ionic charge. Considering an average interionic distance of ~ 1·65–1·67 ± 0·02 Å, the value of N in $(PEG)_x : NH_4NO_3$ can be calculated from the molecular weights and densities of PEG and NH_4NO_3, respectively, yielding $N \sim 1{\cdot}4 \times 10^{26}$ m^{-3}. Activation energy, E_a (NMR), obtained from the plot of $\ln\tau_c$ vs $1000/T$ and hence σ(NMR) calculated using (2) are tabulated and compared with values obtained from complex impedance spectroscopy in table 2. As seen from the table, σ(NMR) is much higher than that measured from the complex impedance plot. Such discrepancies have been observed earlier in the literature. This could be because of the sensitivity of NMR to local dynamics in contrast with the conductivity measurement, which measures only the long-range transport. Another reason for this difference could be that while conductivity measurement responds to the motion of only charged (i.e. dissociated) species, NMR can sense the motion of undissociated molecules as well. Such differences in the conductivities determined by the two techniques have been discussed earlier (Brinkmann 1992).

3.4 *Ionic conductivity measurements*

The ionic conductivity as a function of salt concentration (mole fraction) for $(PEG)_x : NH_4NO_3$ at 300 K is shown in

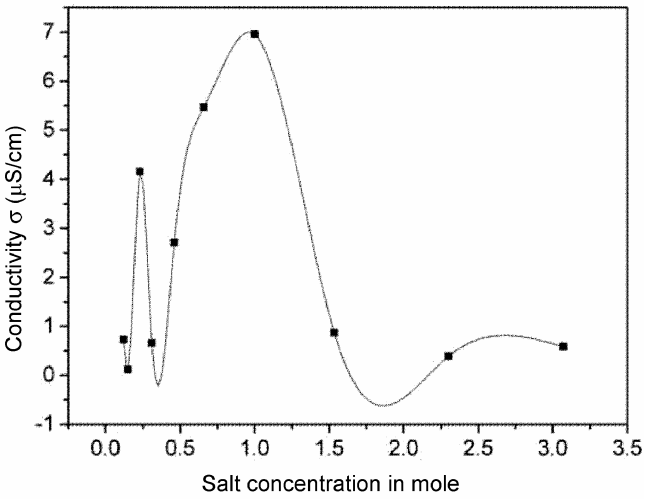

Figure 6. Variation of ionic conductivity with salt concentration in $(PEG)_x : NH_4NO_3$ system.

Table 2. Results of NMR parameters obtained from ^{1}H NMR line widths for $(PEG)_x : NH_4NO_3$.

x value	τ_o (s)	E_a (NMR) (eV)	τ_c at 300 K (s)	σ(NMR) (S/cm)	σ (S/cm)
15	$7{\cdot}1 \times 10^{-13}$	0·32	$1{\cdot}82 \times 10^{-7}$	$3{\cdot}00 \times 10^{-4}$	$0{\cdot}59 \times 10^{-6}$
46	$1{\cdot}7 \times 10^{-11}$	0·30	$1{\cdot}69 \times 10^{-6}$	$3{\cdot}21 \times 10^{-5}$	$6{\cdot}96 \times 10^{-6}$
70	$2{\cdot}3 \times 10^{-11}$	0·28	$9{\cdot}05 \times 10^{-7}$	$6{\cdot}02 \times 10^{-5}$	$5{\cdot}47 \times 10^{-6}$

Table 3. Arrhenius and VTF equations fitting parameters for $(PEG)_{70} : NH_4NO_3$.

x value	Salt (mole)	E_a (eV)	T_c (K)	A ($SK^{0.5}$ cm^{-1})	B (eV)	T_0 (K)
70	0·657	0·83	308	0·37	0·089	176·8

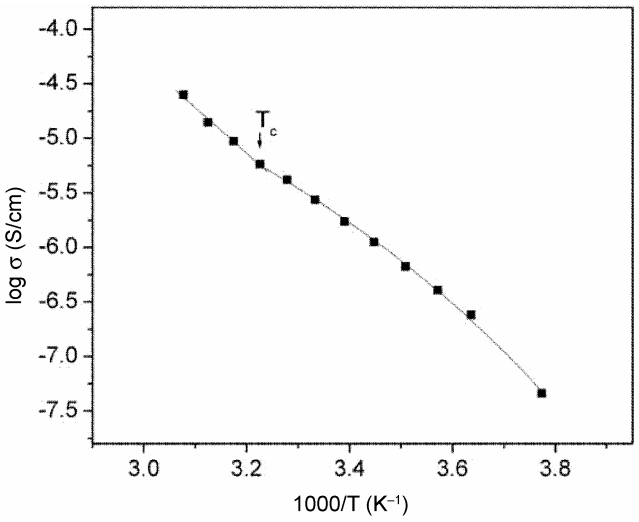

Figure 7. Conductivity vs temperature plot for $(PEG)_{70}$: NH_4NO_3. The solid lines are fits to the Arrhenius (above T_c) and the VTF (below T_c) equations.

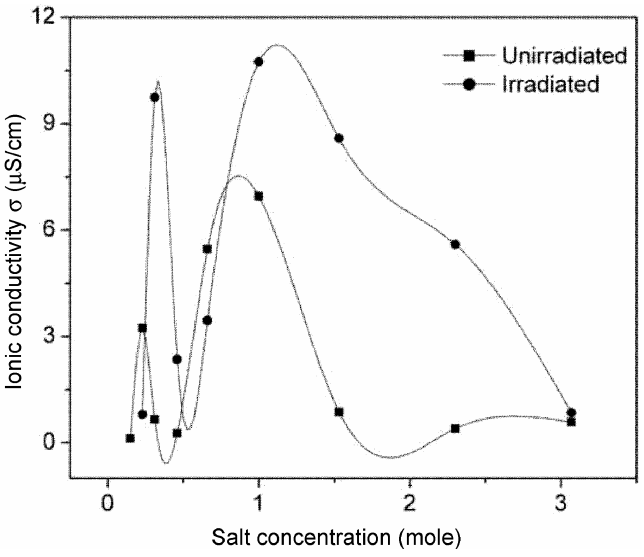

Figure 8. Ionic conductivity vs salt concentration for electron beam irradiated $(PEG)_x : NH_4NO_3$ system.

figure 6. The conductivity isotherm shows a characteristic double peak. At low salt concentrations, the addition of more salt results in an increased ionic conductivity up to a maximum value ($6{\cdot}9 \times 10^{-6}$ S/cm, for $x = 46$). But a further addition of salt causes a decrease in conductivity (Gray 1991). The initial increase in conductivity in the low concentration systems is explained as due to the increase in charge carriers as the number of free cations increases and also a decrease in X_c with an increase in salt concentration. The further decrease in σ though X_c decreases further at higher salt concentration could be due to an increase in the ion–ion interaction that impedes the motion of NH_4^+ and the stiffening of polymer chains as a result of cross links formed by cations and salt precipitation (Gray 1991). Also at higher salt concentration, the formation of ionic clusters too causes a decrease in mobility of charge carriers, since these large aggregates migrate slower than free ions because of their size.

Ionic conductivity has also been measured as a function of temperature for a few selected compositions of the salt. Figure 7 shows the variation of conductivity as a function of temperature for $(PEG)_{70} : NH_4NO_3$. The ionic conductivity increases monotonically as the temperature rises and reaches a high value of $\sim 5{\cdot}23 \times 10^{-4}$ S/cm at 330 K. From the temperature dependence experiments, it is seen that there exists a temperature, T_c, below which the conductivity plot has a curvature and above which it linearly and steeply rises till the melting temperature of the sample. The region below T_c fits the empirical Vogel–Tamman–Fulcher (VTF) (Vogel 1922; Tamman and Hesse 1926; Fulcher 1925) equation

$$\sigma = \frac{A}{\sqrt{T}} \exp\left(\frac{-B}{k(T - T_o)}\right), \tag{3}$$

where T is the absolute temperature and T_o the ideal glass transition temperature that is usually 30–50 degrees below T_g i.e. the temperature at which the configurational entropy vanishes, B is an apparent activation energy which is dependent on the free energy barrier opposing configurational rearrangements and A a pre-exponential factor related to the number of carriers (Gibbs and DiMarzio

1958). The fitting parameter values are given in table 3. The Arrhenius equation

$$\sigma = \sigma_o \exp\left(\frac{-E_a}{kT}\right), \quad (4)$$

where the symbols have their usual meanings, fits the region above T_c. The crossover between Arrhenius and VTF behaviour of $\sigma(T)$ is widely reported and discussed in the literature (Ratner 1987; Binesh and Bhat 1998).

3.5 *Effect of electron and gamma irradiation on ionic conductivity*

Figure 8 shows the observed conductivity changes as a function of salt concentration before and after electron irradiation in $(PEG)_x : NH_4NO_3$ system to a dose of 10 kGy. Irradiating with 8 MeV electron beam has resulted in the increase in the ionic conductivity by a factor of 2 to 3. The increase in conductivity is seen in almost all salt compositions. However, the increase is more pronounced in the medium salt concentration range, $x = 46$. The maximum conductivity achieved due to irradiation is $10{\cdot}74 \times 10^{-6}$ S/cm for $x = 46$. Figure 9 shows the observed conductivity changes as a function of salt concentration before and after ^{60}Co γ-irradiation to a dose of 10 kGy. The process of gamma ray irradiation dramatically enhances the ionic conductivity (by one to two orders of magnitude). It is again observed that the conductivity enhancement is seen in almost all salt compositions. However, it is more pronounced in the medium salt concentration range ($x = 46$). The maximum conductivity after γ-ray irradiation is found to be $3{\cdot}32 \times 10^{-5}$ S/cm for $x = 46$. The increase in conductivity after electron beam and gamma irradiation could be due to the increase in the amorphous content of the sample. The electrolyte samples have been irradiated by 8 MeV electrons to three different doses (5, 10 and 15 kGy) and conductivity measurements are made. Ionic conductivity is found to increase by the same order after each accumulated dose. However, conductivity enhancement is found to be maximum after irradiation to an intermediate dose of 10 kGy. The results are thus reported only for the dose of 10 kGy. Conductivity measurements have been carried out over a period ranging from a few hours to several months after irradiation. The observation is that there is hardly any change in the values of conductivity. This would indicate that the irradiation induced effects are permanent in nature.

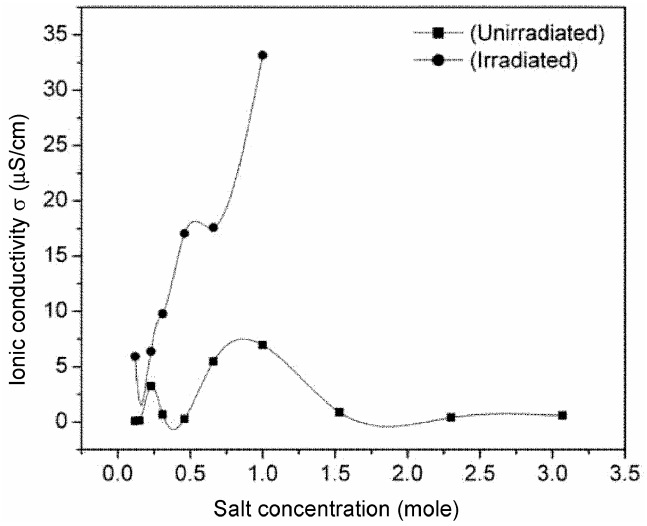

Figure 9. Ionic conductivity vs salt concentration for gamma ray irradiated $(PEG)_x : NH_4NO_3$.

3.6 *Effect of quenching on ionic conductivity*

Figure 10 depicts the observed conductivity changes as a function of salt concentration before and after quenching.

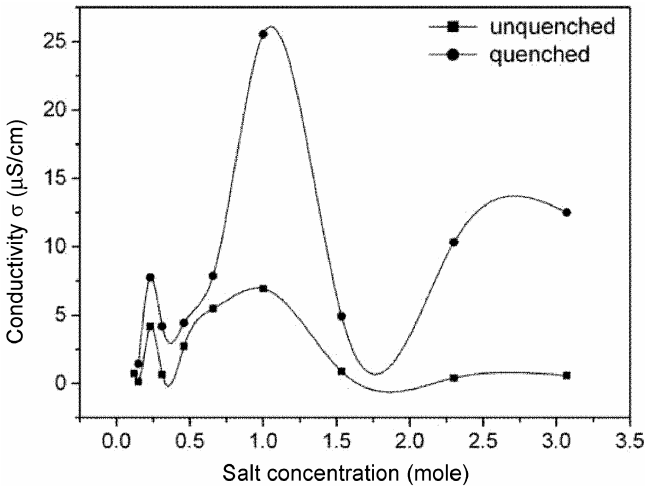

Figure 10. Ionic conductivity vs salt concentration for quenched $(PEG)_x : NH_4NO_3$ system.

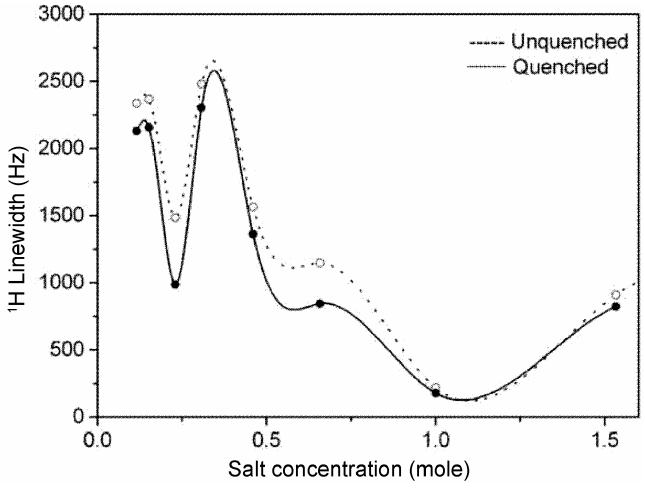

Figure 11. ^{1}H line width as a function of salt concentration for quenched $(PEG)_x : NH_4NO_3$.

Table 4. DSC results of quenched $(PEG)_x : NH_4NO_3$.

		T_m (°C)		T_g (°C)		% Crystallinity (X_c)	
x	Salt content (mole)	Unquenched	Quenched	Unquenched	Quenched	Unquenched	Quenched
15	3·067	53·8	48·7	–63·3	–43·9	61	58
20	2·300	53·9	42·7	–62·8	–45·7	64	62
30	1·533	53·1	50·8	–62·7	–45·3	66	65
46	1·000	53·7	46·5	–66·0	–44·1	67	61
70	0·657	54·4	48·8	–62·8	–49·7	68	66
100	0·460	53·3	50·8	–63·0	–49·3	70	67
150	0·307	–	51·3	–	–	–	–
200	0·230	54·1	50·4	–62·0	–	78	77
300	0·153	–	–	–	–	–	–
400	0·115	54·7	49·2	–58·1	–	79	77
PEG	0·000	55·0	–	–		83	–

The process of quenching enhances the ionic conductivity by one to two orders of magnitudes. The maximum conductivity after quenching is found to be $2{\cdot}56 \times 10^{-5}$ S/cm for $x = 46$. Table 4 shows the DSC results obtained before and after quenching. The DSC studies reveal that increase in the conductivity is more due to the increase in the amorphous content of the system after quenching. The percentage of crystallinity is found to decrease in almost all salt compositions after quenching. ^{1}H NMR line widths have also been recorded at room temperature for both quenched and unquenched systems (figure 11). The process of quenching is found to decrease the line width marginally. The lowest line width is observed for $x = 46$ concentration, for which the quenching process has shown maximum enhancement in ionic conductivity.

4. Conclusions

A new solid polymer electrolyte $(PEG)_x : NH_4NO_3$ has been synthesized, characterized and studied using XRD, DSC, NMR and a.c. conductivity techniques. XRD results confirm the formation of polymer salt complex. The samples with higher salt concentrations are softer and moderately hygroscopic. Samples of intermediate salt concentrations are less hygroscopic and show higher ionic conductivity. The room temperature conductivity is highest ($6{\cdot}97 \times 10^{-6}$ S/cm) for $x = 46$. At low salt concentrations they are highly crystalline and less hygroscopic and have moderate room temperature conductivity of the order of 10^{-7} S/cm. As the salt concentration increases they become more amorphous leading to increase in conductivity. The concentration dependence of conductivity shows characteristic peak for intermediate salt concentration ($x = 46$). The glass transition temperature is minimum for intermediate salt concentration ($x = 46$) and for all other salt concentrations, T_g is higher due to stiffening of the polymer chains due to cross linking among them. T_m of samples is lower than the pure PEG-2000. The degree of crystallinity, X_c, is observed to decrease with an increase in salt concentration. This reduction in X_c is attributed to the lower T_m and decrease in heat of melting, ΔH_m, with the increase in salt concentration. ^{1}H NMR line widths and DSC results are consistent with the room temperature conductivity results.

The ionic conductivity increases monotonically with temperature and reaches a maximum value of $5{\cdot}23 \times 10^{-4}$ S/cm at temperature, 330 K. The temperature dependence of conductivity fits the Arrhenius and VTF equations at different temperature ranges. The process of exposing the solid polymer electrolytes to ionizing radiations like electron beams and gamma rays and quenching to liquid nitrogen temperature gives rise to an increase in conductivity by nearly one order of magnitude. Of the three methods of conductivity enhancement, the gamma ray irradiation appears to be more effective giving rise to maximum conductivity of $3{\cdot}32 \times 10^{-5}$ S/cm for $x = 46$.

Acknowledgements

One of the authors (PNK) thanks the University Grants Commission, Government of India, for a FIP-Teacher Fellowship and financial assistance. The authors thank Prof. A V Chadwick, University of Kent, UK, for his help in DSC measurements. The authors also thank Mr Madhurjya M Borgohain for his help during the conductivity measurements.

References

Armand M B, Chabagno J M and Duclot M J 1979 *Fast ion transport in solids* (eds) P Vashista *et al* (New York: Elsevier North Holland)

Berthier C, Gorecki W, Minier M, Armand M B, Chabagno J M and Rigaud P 1983 *Solid State Ionics* **11** 91

Binesh N and Bhat S V 1999 *Solid State Ionics* **122** 291

Binesh N and Bhat S V 1998 *J. Polym. Sci. Part B: Polym. Phys.* **36** 1201

Brinkmann D 1992 *Prog. NMR Spectrosc.* **24** 527

Fulcher G H 1925 *J. Am. Ceram. Soc.* **8** 339
Gibbs J H and DiMarzio E A 1958 *J. Chem. Phys.* **28** 373
Gray F M 1991 *Solid polymer electrolyte—fundamentals and technological applications* (New York: VCH Inc.)
Haig H I, Herema H R M and Baam B M 2004 *J. Endo Chem.: Phys. Dut. Aspects* 110
Hendrickson J R and Bray P J 1973 *J. Magn. Res.* **9** 341
Hikichi K and Furuichi J 1965 *J. Polym. Sci.* **A3** 3003
Jenkins H D B and Morris D F C 1976 *Mol. Phys.* **32** 231
Johansson A, Wendsjö A and Tegenfeldt J 1992 *Electrochim. Acta* **37** 1487
Joykumar Singh T and Bhat S V 2003 *Bull. Mater. Sci.* **26** 707
Le Nest J F, Gandini A and Cheradane H 1988 *Br. Polym. J.* **20** 253
Li X and Hsu S L 1984 *J. Polym. Sci., Polym. Phys. Ed.* **22** 1331
Nader Binesh and Bhat S V 1996 *Solid State Ionics* **92** 261
Ratner M A 1987 in *Polymer electrolyte reviews* (eds) J R MacCallum and C A Vincent (Elsevier Applied Science) **Vol. I**, p. 185
Shi J and Vincent C A 1993 *Solid State Ionics* **60** 11
Tamman V G and Hesse H Z 1926 *Anorg. Allg. Chem.* **19** 245
Vincent C A 1987 *Prog. Solid State Chem.* **17** 145
Vogel H 1922 *Phys. Z.* **22** 645
Watanabe M, Togo M, Sanui K, Ogata N, Kobayashi T and Ohtaki Z 1984 *Macromolecules* **17** 2908